Journal of Cerebral Blood Flow & Metabolism (2013) 33, 348–350

www.jcbfm.com

BRIEF COMMUNICATION

Voxel-based imaging of translocator protein 18kDa (TSPO) in high-resolution PET

Ji Hyun Ko[1,2], Yuko Koshimori[1,2], Romina Mizrahi[1], Pablo Rusjan[1], Alan A Wilson[1], Anthony E Lang[2,3], Sylvain Houle[1] and Antonio P Strafella[1,2,3]

In vivo imaging of translocator protein 18 kDa (TSPO) has received significant attention as potential biomarker of microglia activation. Several radioligands have been designed with improved properties. Our group recently developed an ^{18}F-labeled TSPO ligand, [^{18}F]-FEPPA, and confirmed its reliability with a 2-tissue compartment model. Here, we extended, in a group of healthy subjects, its suitability for use in voxel-based analysis with the newly proposed graphical analysis approach, Relative-Equilibrium-Gjedde-Patlak (REGP) plot. The REGP plot successfully replicated the total distribution volumes estimated by the 2-tissue compartment model. We also showed its proof-of-concept in a patient with possible meningioma showing increased [^{18}F]-FEPPA total distribution volume.

Journal of Cerebral Blood Flow & Metabolism (2013) **33,** 348–350; doi:10.1038/jcbfm.2012.203; published online 2 January 2013

Keywords: inflammation; kinetic modeling; microglia; neurooncology; positron emission tomography

INTRODUCTION

Activated microglia has a pivotal role in neuroinflammation and abundantly expresses a protein in their mitochondria called the translocator protein 18 kDa (TSPO).[1,2] Increased TSPO expression has been shown in different brain diseases such as cerebral ischemia, HIV, encephalitis, Alzheimer's disease, multiple sclerosis, and stroke.[3]

To date, there have been a few attempts to use positron emission tomography (PET) to assess the level of microglial activation. First, [^{11}C]-PK11195 has been used to quantify TPSO expression.[4] However, this radiotracer had several limitations including high nonspecific binding, low brain penetration, high plasma protein binding, and a difficult preparation.[4] Newly developed TSPO tracers that overcame the deficiencies of [^{11}C]-PK11195 include [^{11}C]-PBR28 (ref. 5) and [^{11}C]-DPA713 (ref. 6). Recently, our imaging group has developed a new radiotracer, [^{18}F]-FEPPA (ref. 7) which, while it has overcome some of the previous limitations associated with older tracers, being an ^{18}F-labeled radiotracer (cf., [^{18}F]-DPA714) it has the advantage of wider distribution to imaging sites distant from the production location particularly useful for larger clinical application.

Recently, Rusjan *et al*[8] showed that the 2-tissue compartment model-estimated total distribution volume (V_T) is the most reliable outcome for [^{18}F]-FEPPA quantification. However, because of the heavy computation and high susceptibility to noise, full kinetic modeling is limited to region-of-interest (ROI) analyses where ROIs must be predefined with specific hypothesis. Thus, it would be important to validate a method to estimate V_T in voxel-wise manner which could be useful especially for clinical applications, e.g., where only a small brain region may be affected or no *a priori* hypothesis exists.

In the absence of a reference region (i.e., brain area that expresses negligible binding[9]), graphical approaches may be the only solution to estimate voxel-wise V_T. The Logan plot[10] is the most widely used graphical analysis that estimates V_T, but it underestimates V_T in the presence of noise,[11] and as it requires the tracer kinetics to reach its equilibrium, it may not be suitable for voxel-wise calculation for [^{18}F]-FEPPA. Zhou *et al.*[12] recently proposed the Relative-Equilibrium-Gjedde-Patlak (REGP) method for reliable estimation of voxel-wise V_T for radioligands that reach equilibrium slowly, i.e., it does not require the tracer kinetics to reach its equilibrium. Mathematically, the total distribution volumes estimated by the Logan (DV_L) and REGP plot (DV_{REGP}) are the same if, and only if, the noise in the tissue tracer kinetics is negligible.[12]

In the present study, we have validated the use of the REGP method for [^{18}F]-FEPPA PET in a group of healthy subjects and visualized its proof-of-concept in a patient who had a possible meningioma. Various forms of brain tumors, including meningioma, have been reported to be associated with increased TSPO expression.[13,14]

MATERIALS AND METHODS

Subjects

Fifteen healthy subjects (age 58.9 ± 2.56, mean ± s.e.) and one patient with Parkinson's disease (PD) underwent an [^{18}F]-FEPPA PET and magnetic resonance imaging scan. The PD patient (female, 68-year-old) had taken part in an on-going [^{18}F]-FEPPA PET study but was excluded because of this incidental finding (i.e., possible meningioma). All subjects provided written informed consent after all procedures were fully explained, and were approved by the Center for Addiction and Mental Health Ethics Review Board. The ROI analysis of the healthy subjects was published elsewhere.[8]

Radiochemistry

Details of the [^{18}F]-FEPPA synthesis have been described elsewhere.[7] It is reliably and quickly labeled with [^{18}F] by nucleophilic displacement of a tosylate leaving group in a fast one-step reaction, yielding a sterile, pyrogen-free product after purification and formulation.

[1]Research Imaging Centre, Centre for Addiction and Mental Health, University of Toronto, Toronto, ON, Canada; [2]Division of Brain, Imaging and Behaviour – Systems Neuroscience, Toronto Western Research Institute, UHN, University of Toronto, Toronto, ON, Canada and [3]Movement Disorder Unit, E. J. Safra Program in Parkinson Disease, Toronto Western Hospital, UHN, University of Toronto, Toronto, ON, Canada. Correspondence: Professor AP Strafella, CAMH-Research Imaging Centre, Toronto Western Hospital and Institute, University of Toronto, 399 Bathurst Street, Toronto, ON, Canada M5T 2S8.
E-mail: antonio.strafella@uhnres.utoronto.ca or antonio.strafella@camhpet.ca
This work was supported by Canadian Institutes of Health Research (MOP 110962). APS is also supported through the Canada Research Chair program.
Received 4 September 2012; revised 16 November 2012; accepted 12 December 2012; published online 2 January 2013

Positron Emission Tomography

A dose of 175.5 ± 3.3 MBq (4.74 ± 0.09 mCi) of intravenous [^{18}F]-FEPPA was administered as a bolus for the PET scans (mass 1.03 ± 0.22 μg, range: 0.16 to 3.22). An automatic blood sampling system (ABSS, Model #PBS-101 from Veenstra Instruments, Joure, The Netherlands) was used to measure arterial blood radioactivity levels continuously at a rate of 2.5 mL/min for the first 22.5 minutes. Manual blood samples were obtained at 2.5, 7, 12, 15, 30, 45, 60, 90, and 120 minutes. These samples were used to determine the temporal evolution of the ratio of radioactivity in whole blood to radioactivity in plasma, and the amount of unmetabolized radioligand in plasma needed to create the input function for the kinetic analysis.[8] The scan duration was 125 minutes after the injection of [^{18}F]-FEPPA. The images were reconstructed into 34 time frames. Frames were acquired as followed: 1 frame of variable length, 5 × 30, 1 × 45, 2 × 60, 1 × 90, 1 × 120, 1 × 210, and 22 × 300 seconds. The PET images were obtained using 3D HRRT brain tomography (CPS/Siemens, Knoxville, TN, USA), which measures radioactivity in 207 slices with an interslice distance of 1.22 mm. All PET images were corrected for attenuation using a single photon point source, ^{137}Cs (T50 = 30.2 years, Eg = 662 keV) and were reconstructed by filtered back projection algorithm, with a HANN filter at Nyquist cutoff frequency.

Region of Interest- and Voxel-Based Analyses

For the anatomic delineation of ROIs, a brain magnetic resonance image was acquired for each subject. 2D axial proton density magnetic resonance images were acquired with a General Electric (Milwaukee, WI, USA) Signa 1.5T magnetic resonance image scanner (slice thickness = 2 mm, repetition time > 5,300 milliseconds, echo time = 13 milliseconds, flip angle = 90 degree, number of excitations = 2, acquisition matrix = 256 × 256, and field of view = 22 cm). Regions of interest were automatically generated using the in-house software, ROMI (ref. 15). Briefly, ROMI (CAMH, Toronto, Ontario, Canada) fits a standard template of 29 ROIs to an individual high-resolution proton density magnetic resonance image scan based on the probability of gray matter, white matter, and cerebrospinal fluid.[15] For the detailed description of the ROIs, see ref. 15. The individual magnetic resonance image with ROIs properly superimposed is then coregistered to the summed [^{18}F]-FEPPA PET image using a mutual information algorithm to generate the time activity curves from each ROI. Time activity curves and metabolite-corrected plasma input function were used to estimate the V_T, DV_L, and DV_{REGP} using a 2-tissue compartment model,[8] Logan plot,[10] and REGP plot,[12] respectively. V_T was considered reliable only if its coefficient of variation (COV) was < 15% (ref. 8). In addition, DV_L and DV_{REGP} were also calculated in voxel-by-voxel basis.[10,12] The voxel-wise DV_L and DV_{REGP} were averaged within each ROI for comparisons with V_T estimated by full kinetic analysis results.

To examine if the noise was in fact the source of underestimation in the voxel-based analysis using Logan plot,[11] the voxel-based Logan analysis and regression analysis were repeated with smoothed dynamic PET images (full width at half maximum = (8, 8, 8 mm) and (16, 16, 16 mm)).

The DV_{REGP} map of the PD patient with meningioma was coregistered with the anatomic magnetic resonance imaging then transformed to Montreal Neurological Institute space for visualization. For this patient, binding potential of [^{18}F]-FEPPA is also calculated in the tumor and contralateral region.

Statistical Analysis

All DV_L and DV_{REGP} of both ROI-based and voxel-based analysis were tested for linear regression with V_T estimated by the 2-tissue compartment model

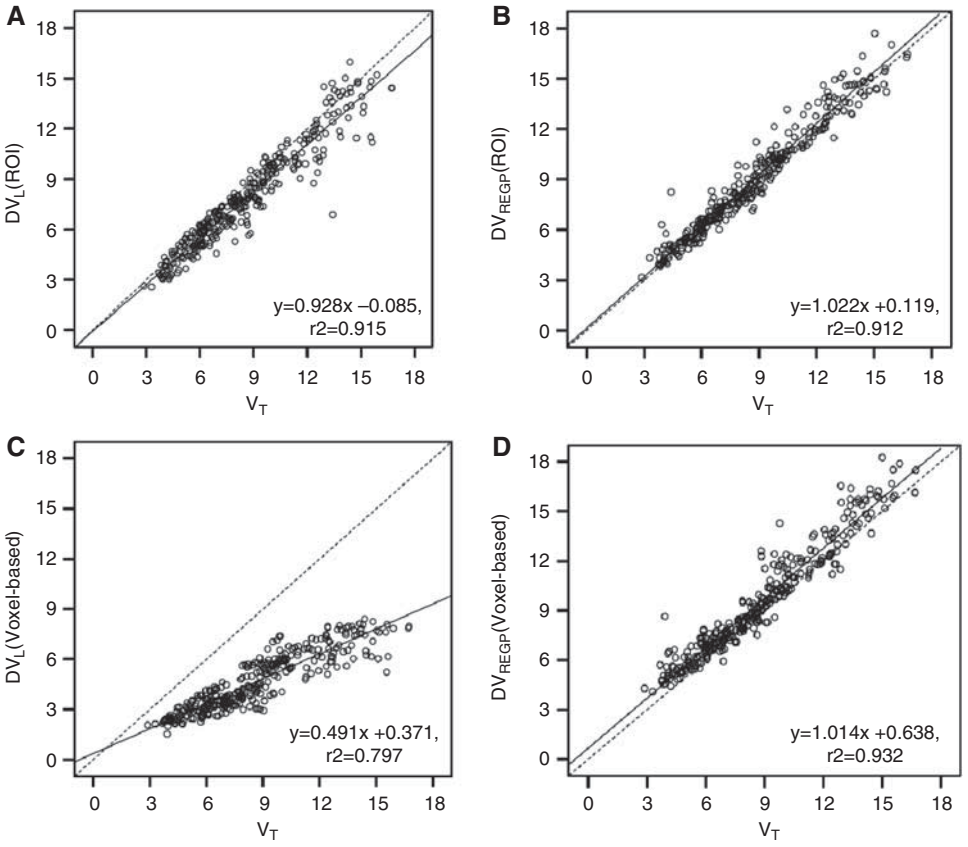

Figure 1. Linear regression of total distribution volume (V_T) estimated by 2-tissue compartment model and graphical approaches. In region of interest (ROI) analysis, (**A**) Logan plot (DV_L) slightly underestimated the slope of regression of V_T calculated by 2-tissue compartment model ($r^2 = 0.915$; $b_0 = -0.085$, $t(326) = -0.586$, $P = 0.558$; $b_1 = 0.928$, $t(326) = -4.5$, $P < 0.001$). (**B**) Relative-Equilibrium-Gjedde-Patlak (REGP) plot (DV_{REGP}) reliably estimated V_T ($r^2 = 0.912$; $b_0 = 0.119$, $t(326) = 0.737$, $P = 0.462$; $b_1 = 1.022$, $t(326) = 1.22$, $P = 0.223$). In voxel-based analysis, (**C**) Logan plot (DV_L) did not reliably estimate V_T ($r^2 = 0.797$, $b_0 = 0.371$, $t(326) = 2.945$, $P = 0.003$; $b_1 = 0.491$, $t(326) = 36.36$, $P < 0.001$), while (**D**) REGP method (DV_{REGP}) reliably predicted V_T ($r^2 = 0.932$; $b_0 = 0.638$, $t(326) = 4.576$, $P < 0.001$; $b_1 = 1.014$, $t(326) = 0.93$, $P = 0.351$). V_T and DV_L were taken from 29 ROIs in 15 healthy subjects (see Materials and methods).

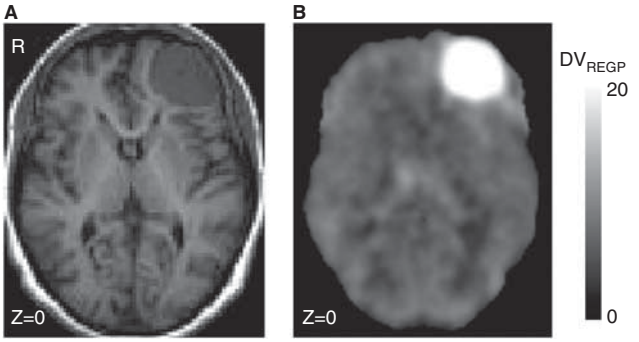

Figure 2. Patient with possible meningioma. (**A**) T1-MRI (**B**) DV_{REGP} of [^{18}F]-FEPPA PET. DV, distribution volume; MRI, magnetic resonance imaging; PET, positron emission tomography; REGP, Relative-Equilibrium-Gjedde-Patlak.

which is the 'gold standard' for [^{18}F]-FEPPA PET quantification.[8] The $r^2 > 0.9$ (i.e., $>90\%$ of variance is explained by regression model) is considered for reliable estimation of V_T. The regression coefficients were also tested as to whether they are significantly different from reference line of $y = x$ (i.e., $b_0 = 0$ and $b_1 = 1$) with a one-sample *t*-test.

RESULTS

In ROI analysis, both DV_L ($r^2 = 0.915$) and DV_{REGP} ($r^2 = 0.912$) reliably estimated the V_T calculated by the 2-tissue compartment model. DV_L slightly underestimated the slope of regression ($b_0 = -0.085$, $t(326) = -0.586$, $P = 0.558$; $b_1 = 0.928$, $t(326) = -4.5$, $P < 0.001$; Figure 1A). In contrast, as also showed by Zhou *et al.*,[12] DV_{REGP} reliably estimated both the slope and intercept of the regression ($b_0 = 0.119$, $t(326) = 0.737$, $P = 0.462$; $b_1 = 1.022$, $t(326) = 1.22$, $P = 0.223$; Figure 1B). This difference was even greater in voxel-based analysis, i.e., DV_L calculated in voxel-by-voxel manner did not reliably estimate V_T ($r^2 = 0.797$, $b_0 = 0.371$, $t(326) = 2.945$, $P = 0.003$; $b_1 = 0.491$, $t(326) = 36.36$, $P < 0.001$; Figure 1C), while voxel-wise DV_{REGP} reliably predicted V_T ($r^2 = 0.932$; $b_0 = 0.638$, $t(326) = 4.576$, $P < 0.001$; $b_1 = 1.014$, $t(326) = 0.93$, $P = 0.351$; Figure 1D).

The underestimation of V_T by DV_L was improved when the dynamic PET images were smoothed with full width at half maximum = 8 mm ($r^2 = 0.865$, $b_0 = -0.225$, $t(326) = -1.303$, $P = 0.193$, $b_1 = 0.860$, $t(326) = -7.368$, $P < 0.001$). However, r^2 was slightly decreased as bigger smoothing kernel was used (full width at half maximum = 16 mm, $r^2 = 0.817$, $b_0 = 0.606$, $t(326) = 3.010$, $P = 0.003$, $b_1 = 0.836$, $t(326) = -7.455$, $P < 0.001$).

The PD patient (Figure 2) was excluded from our on-going research study in PD patients because of an incidental finding of possible meningioma in the left frontal lobe. A full kinetic analysis with input function of the ROI showed that the tumor (left frontal) presented a V_T of 25.1 mL/cm^3 (%COV = 7%), which was three times higher than the contralateral, right frontal side $V_T = 7.6$ mL/cm^3 (%COV = 3.7).

DISCUSSION

We extended the suitability of [^{18}F]-FEPPA PET for use in voxel-based analysis with the newly proposed graphical analysis approach, i.e., REGP plot.[12] The REGP plot successfully replicated the total distribution volumes estimated by the 2-tissue compartment model. The underestimation of slope and r^2 of regression in the voxel-based Logan plot analysis was improved when the dynamic PET image was smoothed, which indicates that the noise in fact was an important source of error. Nevertheless, the highest r^2 of regression was achieved when voxel-based REGP method was used without smoothing ($r^2 = 0.932$).

We also showed its proof-of-concept in a patient with possible meningioma showing increased [^{18}F]-FEPPA total distribution volume. Therefore, voxel-based analysis of [^{18}F]-FEPPA PET may be reliably used for explorative research studies that aim to probe microglia activation *in vivo*.

In the absence of a blocking experiment (as no TSPO drug is approved for human use), it is not possible to know with certainty how much of this binding is specific and how much is free or nonspecific. Moreover, the shape of the TACs is difficult to compare because the delivery in the tumor is different than in regular tissue; K_1 in the tumor ROI was double than that in the right frontal (0.27 (COV = 5%) versus 0.15 (COV = 3%) mL/cm^3 per minute), and there is no evidence to assume that the distribution volumes of the free and nonspecific compartment are the same in the tumor and the right frontal side. However, relying in the best fitting solution for the full kinetic analysis, the tumor presents a binding potential of 9.9 (COV = 9%) which is 57% higher than the contralateral, right frontal binding potential = 6.3 (COV = 8%). Based on the previous reports that TSPO expression is increased in meningioma[13,14] and increased binding of [^{18}F]-FEPPA in the brain region with abundant TSPO expression in rats,[7] our results support the utility of [^{18}F]-FEPPA PET as a valid probe for TSPO *in vivo*.

DISCLOSURE/CONFLICT OF INTEREST

The authors declare no conflict of interest.

REFERENCES

1 Braestrup C, Albrechtsen R, Squires RF. High densities of benzodiazepine receptors in human cortical areas. *Nature* 1977; **269**: 702–704.
2 Kreutzberg GW. Microglia: a sensor for pathological events in the CNS. *Trends Neurosci* 1996; **19**: 312–318.
3 Cosenza-Nashat M, Zhao ML, Suh HS, Suh HS, Morgan J, Natividad R *et al.* Expression of the translocator protein of 18 kDa by microglia, macrophages and astrocytes based on immunohistochemical localization in abnormal human brain. *Neuropathol Appl Neurobiol* 2009; **35**: 306–328.
4 Camsonne R, Crouzel C, Comar D *et al.* Synthesis of N-(C-11) methyl, N-(methyl-1 propyl), (chloro-2 phenyl)-1 isoquinoleine carboxamide-3 (Pk-11195) - a new ligand for peripheral benzodiazepine receptors. *J Labelled Comp Radiopharm* 1984; **21**: 985–991.
5 Fujita M, Imaizumi M, Zoghbi SS, Fujimura Y, Farris AG, Suhara T *et al.* Kinetic analysis in healthy humans of a novel positron emission tomography radioligand to image the peripheral benzodiazepine receptor, a potential biomarker for inflammation. *Neuroimage* 2008; **40**: 43–52.
6 Boutin H, Chauveau F, Thominiaux C, Grégoire MC, James ML, Trebossen R *et al.* ^{11}C-DPA-713: a novel peripheral benzodiazepine receptor PET ligand for *in vivo* imaging of neuroinflammation. *J Nucl Med* 2007; **48**: 573–581.
7 Wilson AA, Garcia A, Parkes J, McCormick P, Stephenson KA, Houle S *et al.* Radiosynthesis and initial evaluation of [^{18}F]-FEPPA for PET imaging of peripheral benzodiazepine receptors. *Nucl Med Biol* 2008; **35**: 305–314.
8 Rusjan PM, Wilson AA, Bloomfield PM, Vitcu I, Meyer JH, Houle S *et al.* Quantitation of translocator protein binding in human brain with the novel radioligand [^{18}F]-FEPPA and positron emission tomography. *J Cereb Blood Flow Metab* 2011; **31**: 1807–1816.
9 Lammertsma AA, Hume SP. Simplified reference tissue model for PET receptor studies. *Neuroimage* 1996; **4**: 153–158.
10 Logan J, Fowler JS, Volkow ND, Wolf AP, Dewey SL, Schlyer DJ *et al.* Graphical analysis of reversible radioligand binding from time-activity measurements applied to [N-^{11}C-methyl]-(-)-cocaine PET studies in human subjects. *J Cereb Blood Flow Metab* 1990; **10**: 740–747.
11 Slifstein M, Laruelle M. Models and methods for derivation of *in vivo* neuroreceptor parameters with PET and SPECT reversible radiotracers. *Nucl Med Biol* 2001; **28**: 595–608.
12 Zhou Y, Ye W, Brasic JR, Wong DF. Multi-graphical analysis of dynamic PET. *Neuroimage* 2010; **49**: 2947–2957.
13 Ferrarese C, Appollonio I, Frigo M, Gaini SM, Piolti R, Frattola L. Benzodiazepine receptors and diazepam-binding inhibitor in human cerebral tumors. *Ann Neurol* 1989; **26**: 564–568.
14 Black KL, Mazziotta JC, Becker DP. Brain tumors. *West J Med* 1991; **154**: 186–197.
15 Rusjan P, Mamo D, Ginovart N, Hussey D, Vitcu I, Yasuno F *et al.* An automated method for the extraction of regional data from PET images. *Psychiatry Res* 2006; **147**: 79–89.